

# Scattering Transform for Intrapartum Fetal Heart Rate Characterization and Acidosis Detection

Václav Chudáček<sup>(1)</sup>, Joakim Andén<sup>(2)</sup>, Stéphane Mallat<sup>(2)</sup>, Patrice Abry<sup>(1)</sup>, Muriel Doret<sup>(3)</sup>

**Abstract**—Early acidosis detection and asphyxia prediction in intrapartum fetal heart rate is of major concern. This contribution aims at assessing the potential of the Scattering Transform to characterize intrapartum fetal heart rate. Elaborating on discrete wavelet transform, the Scattering Transform performs a non linear and multiscale analysis, thus probing not only the covariance structure of data but also the full dependence structure. Applied to a real database constructed by a French public academic hospital, the Scattering Transform is shown to catch relevant features of intrapartum fetal heart rate time dynamics and to have a satisfactory ability to discriminate Normal subjects from Abnormal.

## I. MOTIVATION, RELATED WORKS AND CONTRIBUTIONS

**Context: Intrapartum fetal surveillance.** Electronic fetal surveillance during labor aims at predicting asphyxia and thus at the reduction of subsequent fetal and neonatal mortality and morbidity. In clinical routine, electronic surveillance is based on monitoring cardiocotogram (CTG), i.e., fetal heart rate (FHR) and uterine contractions [1]. CTG is assessed by obstetricians according to FIGO guidelines, which are mostly based on temporal features (baseline estimation, long-term variability, accelerations and decelerations). It is considered that abnormal CTG may suggest deterioration of fetal well-being and requires rapid action by obstetricians (e.g., operative delivery). While CTG monitoring enables detection of intrapartum acidosis with high sensitivity, strict adherence to FIGO rules leads to unnecessary operative delivery decisions for a large number of cases where post-birth exams indicate non-stressed newborns [2]. Reducing the False Positive rate thus constitutes a significant public health stake, as operative deliveries may come with severe immediate or later consequences for both the mother and/or the newborn. In that context, FHR time series analysis beyond FIGO criteria has aroused considerable research efforts (e.g. [3]).

**Related works: Intrapartum fetal heart rate characterization.** Following the seminal work in [4] for adult heart rate characterization, and aiming at going beyond FIGO static temporal and global patterns description by taking into account temporal dynamics (correlations in time), spectral analysis has been massively used for the analysis of intrapartum FHR (e.g., [5]). Essentially, it relies on splitting

the spectrum into frequency bands and measuring the respective amounts of energy in each band. Spectrum estimation for intrapartum FHR however suffers from two important shortcomings: Intrapartum FHR appears much less stationary than adult heart rate does, because of significant baseline variations, the occurrence of decelerations, and, foremost, the frequency band split is lead by well documented respiratory and autonomous nervous system regulation mechanisms in adults, that are both immature and not well document for intrapartum FHR. To avoid the band splitting issue, the paradigm of scale invariance (self-similarity, long memory), has been put forward, that essentially states that all frequencies (or scales) are equally contributing to time dynamics. This naturally leads to the use of multiscale (or wavelet-based) analysis. Wavelet analysis, which can also be read as a time-varying representation of data, explicitly addresses the non-stationarity issue and have thus been significantly used to study intrapartum FHR [6], [7], [8], [9].

Because intrapartum FHR time series display significant departures from Gaussianity, it has also been pointed out that it can be fruitful to go beyond second order statistical analysis (correlation, spectrum estimation). This has been envisaged along two very different directions: Either via the estimation of entropy rates, which combines temporal dynamic to joint probability analyses [10]; or via multifractal analysis that characterizes temporal dynamics fluctuations from a large range of (both positive and negative) statistical orders [6], [7], [8], [9], [11]. Both approaches suffer from severe difficulties in the estimation of joint distributions or of higher moments.

**Goals and Contributions.** In that context, the present contribution aims at exploring the potential of a recently introduced non linear time series analysis tool, referred to as Scattering Transform. [12]. A scattering transform is a non-linear multiscale transform which was shown to be highly effective to classify audio signals, image textures, and to analyze multifractal properties [13], [14]. It computes high order statistical information by iterating on wavelet transforms, as explained in Section II. A database of intrapartum FHR, described in Section III, has been constructed by obstetricians, from selection in a large CTG database collected at *Femme-Mère-Enfant* (Woman-Mother-Child) academic Hospital (HFME), in Lyon France. It contains (15) subjects with abnormal outcomes whose CTG where (correctly) classified by FIGO rules to Abnormal, and (30) subjects with normal outcomes, whose CTG classified by FIGO rules either (correctly) to normal (15 subjects) or (incorrectly) to abnormal (15 subjects). Using this database, the benefits and potentials

Work supported by ANR BLANC 2010 FETUSES 18535, HCL-HFME PHRC, ANR BLAN 0126 01, Advanced ERC 320959

<sup>(1)</sup> CNRS, ENS Lyon, Physics Dept., Lyon, France  
firstname.lastname@ens-lyon.fr

<sup>(2)</sup> CNRS, ENS Paris, Math Dept., Paris, France  
firstname.lastname@ens.fr

<sup>(3)</sup> Femme-Mère-Enfant Hospital, Lyon, France  
muriel.doret@chu-lyon.fr

of scattering transforms for intrapartum FHR characterization are explored in details in Section IV, with emphasis on the analysis of the potential reduction of the False Positive rate.

## II. SCATTERING TRANSFORM

A scattering transform iteratively computes the modulus of complex dyadic wavelet transforms [12]. Let  $X(t)$  denote the time series to analyze. A complex wavelet  $\psi(t)$  is a band-pass filter, supported over positive frequencies. Let  $\psi_j(t) = 2^{-j}\psi(2^{-j}t)$  be the dilation of  $\psi$  by  $2^j$ . A complex dyadic wavelet transform computes the convolution  $X \star \psi_j(t)$  at all scales  $2^j$  and at all times  $t$ .

First order scattering coefficients are defined as the time average of wavelet coefficient modulus:

$$SX(j_1) = 2^{-j_1} \sum_{t=1}^{2^{j_1}} |X \star \psi_{j_1}(t)|. \quad (1)$$

where  $2^{j_1}$  is the signal size. The  $SX(j_1)$  are computed up to a coarsest scale  $j_m < J$ :  $1 \leq j_1 \leq j_m$ .

The information lost by averaging  $|X \star \psi_{j_1}|$  is recovered by computing its wavelet coefficients  $\{|X \star \psi_{j_1}| \star \psi_{j_2}(t)\}_{j_2}$ . The amplitude of these new coefficients is averaged in time at all scales  $2^{j_2}$ , such that:  $2^{j_m} \geq 2^{j_2} > 2^{j_1}$ , and normalized by first order coefficients (1), which defines the second order scattering coefficients:

$$SX(j_1, j_2) = \frac{\sum_{t=1}^{2^{j_2}} \||X \star \psi_{j_1}| \star \psi_{j_2}(t)\|}{\sum_{t=1}^{2^{j_1}} |X \star \psi_{j_1}(t)|}. \quad (2)$$

Since  $2^{j_m} \geq 2^{j_2} > 2^{j_1} \geq 1$ , there are  $j_m$  first order coefficients  $SX(j_1)$  and  $j_m(j_m - 1)/2$  second order scattering coefficients  $SX(j_1, j_2)$ . A scattering transform computes coefficients of any order  $m$  by averaging in time the values of  $m$  successive wavelet convolutions and modulus [12]. In this study, we concentrate on first and second order scattering coefficients which carry the most important signal information for classification and scaling analysis [14], [13].

If  $X(t)$  is a realization of a scaling process, then averaging several realizations of  $SX(j_1)$  computes an expected values which can be shown to decay like  $2^{j_1 H}$  where  $H$  is the Hurst exponent measuring long range second order correlations. In this case, one can also prove [14] that averaging several realizations of  $SX(j_1, j_2)$  yields a function that only depends upon  $j_1 - j_2$  and which decays like  $2^{(j_1 - j_2)z}$ , where this second exponent  $z$  depends upon the scaling properties of higher order moments of  $X$ . It characterizes non-Gaussian behavior and discriminates different types of multiscale processes. In the following, we shall see that it provides relevant information to characterize FHR status.

## III. DATABASE

**Data Collection.** Intrapartum CTG has been routinely monitored at HFME for more than 30 years, continuously for fetus with initial intermediate FHR during labor or with high risk of fetal asphyxia (post-date delivery, intra-uterine growth restriction, diabetes). CTG is currently acquired using scalp electrode STAN 21 or 31 systems, 12bit resolution,

500Hz sampling rate, (STAN, Neoventa Medical, Moelndal, Sweden), that outputs lists of R-peak occurrence in ms  $\{t_n\}_{n=1, \dots, N}$ . Umbilical cord artery acid-base status was also systematically recorded for each newborn, with obstetrician annotations motivating the decision for operative delivery. Labor and delivery were completed according to the STAN clinical guidelines.

**Database.** Subjects have been carefully selected by a referent obstetrician to create a database representative of typically observed CTGs and umbilical cord pH describing fetal acid-status just before delivery. They were grouped into 3 classes:

- i) **FIGO-TN:** 15 fetuses with normal fetal outcome (defined as Apgar score of 10 at 5 minutes of life and arterial cord pH  $> 7.30$ , hence non-acidotic thus healthy) and CTG classified as normal – True Negatives (TN);
- ii) **FIGO-TP:** 15 fetuses with respiratory fetal acidosis (umbilical arterial pH  $< 7.05$ , hence abnormal) and CTG classified as abnormal (hence correctly diagnosing fetal-state as abnormal) – True Positives (TP);
- iii) **FIGO-FP:** 15 fetuses with normal fetal outcome (Apgar score of 10, arterial cord pH  $> 7.30$ , hence healthy), yet with abnormal CTG (hence incorrectly diagnosed as abnormal) – False Positives (FP).

**Preprocessing.** As often done in intrapartum FHR characterization [15], [16], the lists of R-peaks were transformed into regularly sampled beat-per-minute (bpm) time series,  $X(t)$ , by linear interpolation of the measurements  $\{(t_n/1000, 60000/(t_{n+1} - t_n))\}_{n=1, \dots, N}$ . The sampling frequency was set to  $f_s = 8$  Hz, FHR can be checked to carry no significant information beyond 3 to 4Hz. Interpolation at higher  $f_s$  has been observed to yield no improvement in classification.

## IV. SCATTERING OF INTRAPARTUM FETAL HR

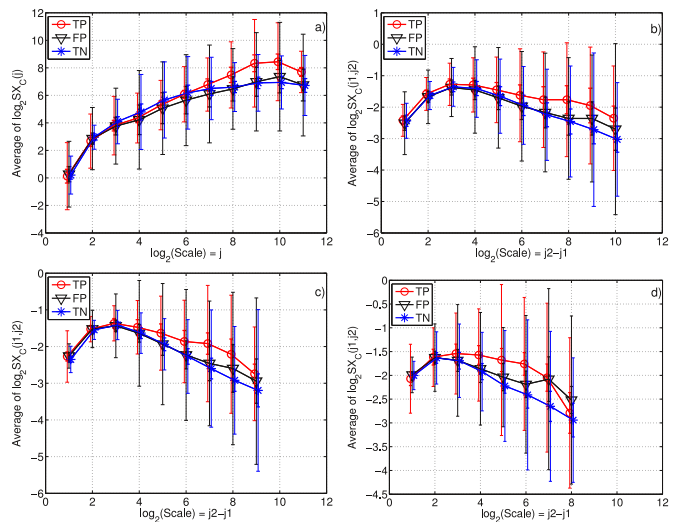


Fig. 1. Average of  $\log_2 SX_c(j_1)$  versus  $j_1$  (a) and of  $\log_2 SX_c(j_1, j_2)$  versus  $j_2 - j_1$ , for  $j_1 = 1$  (b),  $j_1 = 2$  (c),  $j_1 = 3$  (d), computed over 15 realizations for each  $c = \text{FIGO-TN, FIGO-TP, FIGO-FP}$ . Thick error bars corresponds to  $\pm 1$  standard deviation, measured within classes, while the thin error bars corresponds to the extreme observations within each class.

TABLE I  
CORRELATION BETWEEN SCALING EXPONENTS.

C	$\hat{H}_c^S, H_c^L$	$\hat{H}_c^S, \hat{z}_c(1)$	$\hat{H}_c^S, \hat{z}_c(2)$	$\hat{H}_c^S, \hat{z}_c(3)$
FIGO-TP	$\rho = 0.96$	$\rho = 0.73$	$\rho = 0.57$	$\rho = -0.13$
FIGO-FP	$\rho = 0.87$	$\rho = 0.57$	$\rho = 0.01$	$\rho = 0.25$
FIGO-TN	$\rho = 0.83$	$\rho = 0.66$	$\rho = 0.77$	$\rho = 0.66$

TABLE II  
RANKSUM TESTS: P-VALUES

c	$\hat{H}_c$	$\hat{z}_c(1)$	$\hat{z}_c(2)$	$\hat{z}_c(3)$
TP/TN	0.00	0.00	0.00	0.02
TP/FP	0.00	0.01	0.01	0.09
FP/TN	0.02	0.17	0.25	0.15

**Analysis parameters.** To assess the ability of scattering to characterize acidosis, the present study concentrates, for each of the  $3 \times 15$  subjects, on the last 30-minute before delivery, corresponding to  $2^J$  samples. Scattering coefficients are computed, using a complex cubic spline wavelets [12], at scales  $2^{j_1}$  and  $2^{j_2}$ ,  $1 \leq j_1 < j_2 \leq j_m < J$ , where  $2^{j_m} = 2^{11}$  corresponds to  $2^{11}/F_s = 256s \approx 4$  min, considered as a typical time analysis unit by obstetricians and as a satisfactory trade-off between time resolution and stability in estimation. There are thus  $j_m = 11$  first order coefficients  $SX(j_1)$  and  $j_m(j_m - 1)/2 = 55$  second order coefficients  $SX(j_1, j_2)$ .

The set of signals of each class  $c = \text{FIGO-TN, FIGO-TP, FIGO-FP}$  are considered realizations of a random process  $X_c(t)$ . Fig. 1 displays averages of  $SX_c(j_1)$  and  $SX_c(j_1, j_2)$  across each of the classes  $c$ , in log-log coordinates, by analogy to scale invariance analysis.

**Scaling Analysis.** Fig. 1 (a) shows that for each of the 3 classes, the averages of  $SX_c(j_1)$  behave as  $SX_c(j_1) \sim 2^{j_1 H_c}$  for  $2 \leq j_1 \leq 10$ , where  $H_c$  denotes the Hurst exponent for class  $c$ . It also shows, (b), (c) and (d), that  $SX_c(j_1, j_2) \simeq 2^{(j_2 - j_1)z_c(j_1)}$ , for  $3 \leq j_2 - j_1 \leq 8$ . It correspond to time scales ranging from  $2^{j_1}/f_s \times 2^3$  to  $2^{j_1}/f_s \times 2^8$ . For example, with  $j_1 = 2$ , scaling exists in the range 4 to 128s, thus matching the scaling range observed for averages of  $SX_c(j_1)$ . This suggests to compute, by means on linear regression, for the FHR times series of each subject of the 3 classes, the estimates  $\hat{H}_c^S$  and  $\hat{z}_c(j_1)$  for  $j_1 = 1, \dots, j_m$ .

For the same data and under same conditions, the Hurst exponents has also been estimated with the wavelet-Leader multifractal analysis tool detailed in [6]:  $\hat{H}_c^L$ . Estimates  $\hat{H}_c^S$  and  $\hat{H}_c^L$  show high correlation coefficients (cf. Table I, first column) and are found consistently to take values above 0.8 for all 3 classes, thus showing significant long range correlations. This corroborates the analysis already reported on this same database in [7], [8], [9].

As can also be seen in Table I, columns 2 to 4, correlation coefficients between  $\hat{H}_c^S$  and  $\hat{z}_c(j_1)$  are low, thus indicating clearly that the  $SX_c(j_1, j_2)$  conveys information related to high order dependence structure of intrapartum FHR that are not provided by the first order  $SX_c(j_1)$ , which only depends upon the covariance and hence upon second order moments.

The analysis reported above shows that the scaling exponents  $\hat{H}_c$  and  $\hat{z}_c(j_1)$  measured for each subject independently, are robust features, *probing* the scaling properties of the dependence structure of intrapartum FHR time series, and thus extending the Hurst parameter related to scaling of the sole covariance structure.

**Intrapartum FHR classification.** Fig. 1 also indicates that the scattering coefficients of Class FIGO-FP tend to be closer to that of Class FIGO-TN than to that of Class FIGO-TP, a much desired property that tend to suggest that scaling exponents  $\hat{H}_c$  and  $\hat{z}_c(j_1)$  may help in Intrapartum FHR classification. To quantify that observation, boxplots for  $\hat{H}_c^S$  and  $\hat{z}_c(j_1 = 2)$  are shown in Fig. 2 (a) and (b), complemented with Table II that reports the p-values of Wilcoxon rank sum tests, aiming at rejecting equality in mean for the  $\hat{H}_c^S$  and  $\hat{z}_c(j_1)$  for different pairs of classes. Boxplots and p-values clearly indicates that, for any estimated scaling exponents, Class FIGO-FP resembles more to Class FIGO-TN than to Class FIGO-TP.

Experimentally, it is found that, amongst the second order scaling exponents  $\hat{z}_c(j_1)$ ,  $j_1 = 2$  yield the best classification (showing the larger p-value for the pair FIGO-TN/FIGO-FP with low p-value for the pair FIGO-TP/FIGO-FP). Therefore, Fig. 2 (bottom left) displays the scatter plot  $\hat{H}_c^S$  versus  $\hat{z}_c(2)$ , for all subjects of the 3 classes: It clearly shows that Class FIGO-TP lives in the top right corner while Class FIGO-TN seats in the bottom left corner. A significant number of FIGO-FP subjects stand close to Class FIGO-TN subjects.

For classification performance evaluation, given the small number of subjects within each class, the recourse to advanced classification schemes (such as SVM, Logistic Regression or PCA based procedures) fed by the vectors of features  $\hat{H}_c^S$  and  $\hat{z}_c(j_1)$  for each class, appears inappropriate. Instead, for this case study analysis, classification performance are quantified in the  $\hat{H}_c^S$  versus  $\hat{z}_c(2)$  plot, by considering that the Abnormal domain has a shape arbitrarily chosen to be a rectangle. Thus, varying the shape and size of the upper right rectangular Abnormal domain permits to obtain the ROC Curve reported in Fig. 2 (bottom right). It quantifies classification performance in terms of the probability  $p_D$  of correct detection, or sensitivity, of Abnormal subjects (corresponding to Class FIGO-TP) against the probability of False Alarms,  $p_{FA}$ , on incorrect detection of Normal subjects, or  $1 - \text{specificity}$ , (corresponding to Classes FIGO-TN and FIGO-FP). This ROC Curve indicates very satisfactory performance: The curve lives close to the upper left corner (the Golden standard); The most difficult case ( $p_D = 1$ , i.e., all Abnormal subjects are detected - a stringent requirement of clinicians) yields a  $p_{FA} = 0.26$ , which already significantly outperforms the  $p_{FA} = 0.50$  obtained from FIGO-rules for the same database.

## V. CONCLUSIONS AND FUTURE WORKS

In the present contribution, it has been shown that the joint use of only two scattering features  $\hat{H}_c^S$  and  $\hat{z}_c(j_1)$  achieves a satisfactory characterization of intrapartum FHR and efficient discrimination between Normal and Abnormal subjects.

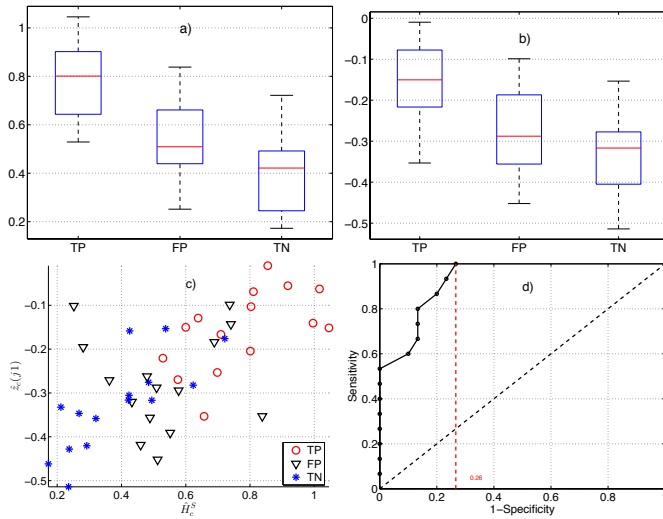


Fig. 2. **Classification Performance.** Box plots (top row) for  $\hat{H}_c^S$  (a) and  $\hat{z}_c(j_1 = 2)$  (b). Within each boxplots, Classes are from left to right: FIGO-TP, FIGO-FP, FIGO-TN. Scatter plot (c) of all subjects of the 3 classes for in the  $\hat{H}_c^S$  versus  $\hat{z}_c(j_1 = 2)$  domain and corresponding ROC Curve (d).

These features that consist of scaling exponents, measured from the scattering coefficients  $SX(j_1)$  and  $SX(j_1, j_2)$ , thus confirm that scaling is a central property enabling to characterize intrapartum FHR time dynamics and enrich scaling analysis: While first order scattering coefficients essentially permits to measure Hurst exponent, second order coefficients significantly enrich scaling analysis by enabling to quantify scaling behaviors in the full dependence structure.

The results obtained from this small-size database are promising. Further we are planning to develop this work along different lines. First, as can be seen in Fig. 2 (bottom right), a number of Normal subjects remain misclassified. Comparisons against other features (FIGO-based; entropy-based [10]; multifractal-based [9]) will be undertaken to see whether, besides overall classification performance, the misclassified subjects are always the same or differ, when using different types of features. Additionally mis-classifications related to specific types of features will be correlated to obstetricians annotations, to establish sub-classes of false positives. Concentrating on the FIGO-FP subjects that are not correctly classified using the scattering, might help to figure out what property can actually discriminate the time dynamics of such cases from that of actually Abnormal subjects and to assess the role of decelerations in the difficulty to correctly classify them. Second, instead of focusing on the last 30 minutes before delivery, the Scattering Coefficients will be computed along time, within sliding windows of duration of 10 to 20 minutes. The optimal duration will be studied in a systematic manner as the outcome of the following trade-off: Obstetricians seek for shorter decision time, but too short time window yields poorer estimation and thus poorer classification performance. Third, the information measured by the  $j_m$  first order coefficients  $S(j_1)$  and  $j_m(j_m - 1)/2$  second order coefficients  $S(j_2)$  have been so far summarized into the sole scaling exponents  $\hat{H}_c^S$  and

$\hat{z}_c(j_1)$ , so that classification can be achieved by the joint thresholding of those quantities, with no a priori reference to a training set. We will however also study the whole set of scattering coefficients as features used to feed more advanced classification procedures. Fourth, scattering will be applied to the classification of a very large database ( $\sim 4000$  subjects) being currently gathered at HFME, Lyon. In that context, the small-size database studied here, will be considered as the training set for the classification of the much larger database and more advanced classification procedure will be used.

## REFERENCES

- [1] E. Chandrharan and S. Arulkumaran, "Prevention of birth asphyxia: responding appropriately to cardiocotograph (ctg) traces," *Best Pract. Res. Clin. Obstet. Gynaecol.*, vol. 21, pp. 609–624, 2007.
- [2] I. Amer-Wahlin, C. Hellsten, H. Hagberg, A. Herbst, I. Kjellmer, H. Lilja, C. Mansson, L. Martensson, P. Olofsson, A. Sundstrom, and K. Marsál, "Cardiotocography only versus cardiotocography plus st analysis of fetal electrocardiogram for intrapartum fetal monitoring: a swedish randomised controlled," *Trial. Lancet.*, vol. 358, no. 9281, pp. 534–538, 2001.
- [3] B.D. Fulcher, A.E. Georgieva, C.W.G. Redman, and N.S. Jones, "Highly comparative fetal heart rate analysis," in *Engineering in Medicine and Biology Society (EMBC), 2012 Annual International Conference of the IEEE*, 28 2012-sept. 1 2012, pp. 3135–3138.
- [4] S. Akselrod, D. Gordon, F. A. Ubel, D. C. Shannon, A. C. Berger, and R. J. Cohen, "Power spectrum analysis of heart rate fluctuation: a quantitative probe of beat-to-beat cardiovascular control," *Science*, vol. 213, no. 4504, pp. 220–222, 1981.
- [5] J. Van Laar, M. Porath, C. Peters, and S. Oei, "Spectral analysis of the fetal heart rate variability for fetal surveillance: review of the literature," *Acta Obstetrica et Gynecologica*, vol. 87, pp. 300–306, 2008.
- [6] H. Wendt, P. Abry, and S. Jaffard, "Bootstrap for empirical multifractal analysis," *IEEE Signal Proc. Mag.*, vol. 24, no. 4, pp. 38–48, 2007.
- [7] P. Abry, H. Helgason, P. Gonçalves, E. Pereira, P. Gaucherand, and M. Doret, "Multifractal analysis of ECG for intrapartum diagnosis of fetal asphyxia," in *Proceeding of the IEEE Int. Conf. on Acoust. Speech and Sig. Proc. (ICASSP), Dallas, USA*, 2010.
- [8] P. Abry, H. Wendt, S. Jaffard, H. Helgason, P. Gonçalves, E. Pereira, Cl. Gharib, P. Gaucherand, and M. Doret M. Doret Cl. Gharib, P. Gaucherand, "Methodology for multifractal analysis of heart rate variability: From LF/HF ratio to wavelet leaders," in *Proceeding of the IEEE Engineering in Medicine and Biology Conference. (IEEE EMBS), Buenos Aires, Argentina*, 2010.
- [9] M. Doret, H. Helgason, P. Abry, P. Gonçalves, Cl. Gharib, and P. Gaucherand, "Multifractal analysis of fetal heart rate variability in fetuses with and without severe acidosis during labor," *Am. J. Perinatol.*, vol. 28, no. 4, pp. 259–266, 2011.
- [10] M. Cost, A. L. Goldberger, and C-K. Peng, "Multiscale entropy analysis of biological signals," *Phys Rev E Stat Nonlin Soft Matter Phys*, vol. 71, no. 2 Pt 1, pp. 021906, Feb 2005.
- [11] R. F. Leonarduzzi, G. Schlotthauer, and M. E. Torres, "Wavelet leader based multifractal analysis of heart rate variability during myocardial ischaemia," in *Proc. 32nd Annual International Conference of the IEEE Engineering in Medicine and Biology Society (EMBC 2010)*, 2010, pp. 110–113.
- [12] S. Mallat, "Group invariant scattering," *Pure and Applied Mathematics*, vol. 10, no. 65, pp. 1331–1398, 2012.
- [13] J. Anden and S. Mallat, "Multiscale scattering for audio classification," in *Proc. ISMIR, New-York*, 2011, vol. 103.
- [14] J. Bruna, "Scattering representation for recognition," *PhD Thesis*, 2012.
- [15] P. Hopkins, N. Outram, N. Lofgren, E. Ifeakor, and K. Rosen, "A comparative study of fetal heart rate variability analysis techniques," in *Proc. of the 28th IEEE EMBS Conf.*, 2006, pp. 1784–1787.
- [16] J. Van Laar, M. Porath, C. Peters, and S. Oei, "Spectral analysis of the fetal heart rate variability for fetal surveillance: review of the literature," *Acta Obstetrica et Gynecologica*, vol. 87, pp. 300–306, 2008.